Performance of the Obese GHBMC Models in the Sled and Belt Pull Test Conditions

Bronislaw D. Gepner, Hamed Joodaki, Zhaonan Sun, Mohan Jayathirtha, Taewung Kim, Jason L. Forman, Jason R. Kerrigan

Abstract

Obesity is associated with an increased fatality risk in automobile collisions. The goal of this study was to evaluate the predictive capabilities of the obese human body models via comparison of model simulations to post-mortem human subject tests from the literature. First, obese post-mortem human subject sled tests were used to assess the ability of the obese GHBMC models to replicate occupant kinematics in a sled environment. Second, lap belt pull tests were used to evaluate belt interaction with the abdomen and pelvis. Third, adipose tissue-level tests were used to evaluate the shear stiffness of the flesh material model used in the obese human body models. Similar to the post-mortem human subject tests, the obese human body models experienced substantial lower extremity forward motion in the sled test simulations. However, the model did not exhibit submarining behaviour as observed in the post-mortem human subject experiments. Further, the lap belt pull simulations failed to reproduce the belt/abdomen interaction seen in the post-mortem human subject, and the material model used to represent the human body model flesh was found to be approximately one order of magnitude stiffer than human abdominal subcutaneous adipose tissue. This study shows that improved models of abdominal flesh, and specifically subcutaneous adipose tissue, may be required to obtain biofidelic belt/abdomen interactions and to predict submarining behaviour in crash simulations.

Keywords: obese, rear-seat, PMHS, GHBMC, restraint, submarining

I. INTRODUCTION

Obesity is a growing socioeconomic problem. According to the World Health Organization (WHO) worldwide obesity has nearly tripled since 1975. In 2016, over 650 million adults and about 380 million children and adolescents were classed as obese. The simplest measure of obesity is defined as Body Mass Index (BMI), a proportion of body mass to the square of one's height (kg/m^2). The WHO defines the normal range of BMI as 18.5-24.9, overweight as 25-29.99 and obese as 30 and above. In 2016, 13% of adults worldwide aged 18 years and over had BMI of more than 30 kg/m^2 [1].

In automobile crashes, obesity is associated with an increased fatality risk [2-5]. When injured, obese occupants suffer more complications, require longer stays in the hospital, more days of mechanical ventilation, and are at increased risk of death compared to non-obese occupants [6-7]. Obesity has also been found to affect the distribution of occupant injuries in automobile crashes. Several researchers found that obese occupants are more likely to sustain lower extremity injuries [8-10], as well as chest injuries [2] [8-10].

In recent years several studies have examined the effect of obesity on occupant restraint engagement and occupant kinematics in vehicle crashes. References [11-12] performed a series of rear-seat sled tests, investigating a 3-point belt with a pretensioner and a progressive force-limiter, on both obese and 50th percentile adult male Post Mortem Human Subjects (PMHSs). Comparing obese and non-obese PMHSs, the authors found substantial differences in kinematics including significantly greater forward motion of the head and the pelvis by the obese occupants. Additionally, the authors observed that the obese occupants exhibited backward torso rotation (pelvis forward of shoulders) at the time of maximum forward excursion, whereas non-obese occupants did not. Seat belt fit for obese occupants using a laboratory setup was also investigated by [13]. They found that the obese group used an increased webbing length, and positioned their lap belt further forward and higher relative to the anterior-superior iliac spines (ASIS) compared to non-obese occupants.

Furthermore, several computational studies on obese occupant-restraint interaction were conducted by the same research group [14-17]. Reference [14] investigated the effect of obesity on occupant injury using the rigid

B. D. Gepner is a Research Scientist (+1-434-297-8046 / bgepner@virginia.edu), H. Joodaki is a PhD student in Mechanical Engineering, Z. Sun is a PhD student in Mechanical Engineering, M. Jayathirtha is an MSc student in Mechanical Engineering, J. L. Forman is a Principal Scientist, J. R. Kerrigan is an Assistant Professor of Mechanical and Aerospace Engineering at University of Virginia, USA. T. Kim is an Assistant Professor at the Mechanical Engineering Department at Korea Polytechnic University, Republic of Korea.

body human body model (HBM), and concluded that the changes in torso/seat belt interaction, along with the increased mass of the occupant, increased the risk of lower extremity injuries. References [15-17] utilised some rapid mesh morphing tools along with statistical models of external body contour and ribcage geometry to generate finite element (FE) HBMs with varied stature, age and BMI levels. This effort was carried out for both Total Human Model for Safety (THUMS) [15-16], and Global Human Body Models Consortium (GHBMC) [17]. The GHBMC effort resulted in the generation of twelve HBMs with different anthropometry (1,750 mm and 1,880 mm), age (30 and 70 year old) and BMI (25, 30, and 35) levels (Fig. 1). The developed models included only geometrical variations and no material properties of tissues were adjusted. Reference [18] performed a series of simulations on the obese THUMS model. The model was validated against the available sled test data and compared against a non-obese model in frontal and side impact scenarios. For the obese model the authors observed a greater forward excursion in a frontal impact, however no submarining behaviour, where a properly-placed belt would have slid over the iliac crests and then would have penetrated into the abdomen without engaging the pelvis, was discussed.

Seat belt fit, along with the lack of pelvis engagement was identified by several researchers as a primary factor responsible for altered kinematics for obese occupants involved in vehicle crashes [11-13] [19]. Reference [12] pointed out that obese PMHSs in frontal-impact sled tests exhibited submarining behaviour. The authors suggested that submarining resulted in increased forward excursion and decreased forward torso pitch, which may be related to increased risk of lower extremity and thoracic injuries in obese occupants. While there are several HBMs available to study occupant kinematics and the sensitivity to submarining, simulations illustrating HBM responses similar to what was seen in the PMHS tests are not available in the literature. As a result, it remains unclear whether the HBMs can be used to accurately replicate the effects that obesity has on lap belt interaction with the abdomen and pelvis. Our hypothesis is that there is a fundamental limitation in the ability of the obese GHBMC models to accurately represent abdomen/lap belt interaction due to the manner in which superficial soft tissue is represented in the models. Thus, the goal of this study is to investigate the interaction between the GHBMC obese occupant models and the lap belt, relative to available material property and obese PMHS testing in the literature to determine if additional development is needed before these models can be used to explore and evaluate injury countermeasures for obese occupants.

II. METHODS

The obese GHBMC models, developed by [17] were evaluated with respect to the available PMHS studies. Three studies, useful for this purpose, were identified. First, our previous obese PMHS sled tests, described by [11], were used to assess the ability of the obese GHBMC models to replicate occupant kinematics in a sled environment. Second, our previous lap belt pull tests, described by [20], were used to evaluate belt interaction with the model's abdomen and pelvis. Third, the adipose tissue-level tests [21], were used to evaluate the shear stiffness of the flesh material model used in the obese HBMs.

Sled Test Simulations

The first part of this study was aimed at evaluating the biofidelity of obese GHBMC models by comparing their kinematics with obese PMHSs in frontal sled tests. The PMHS tests were performed previously at University of Virginia Center for Applied Biomechanics (UVa-CAB) and the results were published in [11, 19]. Briefly, two obese PMHS tests were used as the subjects for frontal sled tests at two different speeds (29 and 48 km/h) in the sled buck created from a rear seat of a sedan. The weight (124 kg) and BMI (35 kg/m^2) of one of the obese GHBMC models matched with those of an obese PMHS (Fig. 1). The 70 years old GHBMC model matching the subject anthropometry was chosen for the comparison purpose (Table 1).

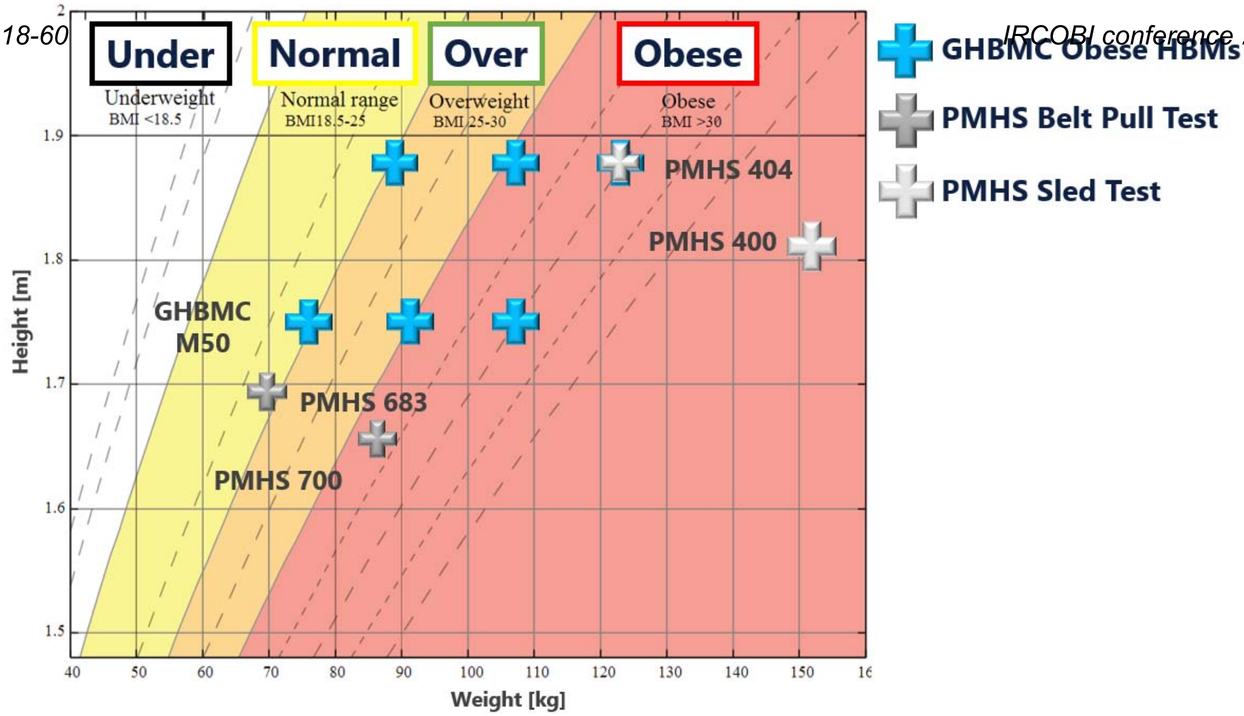

Fig. 1. Anthropometries of the obese GHBMC models and PMHSs from selected studies [11, 17, 20].

TABLE 1
ANTHROPOMETRIES OF THE SELECTED OBESE GHBMC MODELS AND PMHSS FROM SELECTED STUDIES [11, 17, 20].

	PMHS				GHBMC		
Subject #/Test Type	404	400	683	700	M50	Sled	Belt Pull
Height (cm)	189	182	168	165	175	188	175
Weight (kg)	124	151	68	84.4	77.0	118	86
Target BMI	-	-	-	-	25.7	35	30
BMI	35	45	24.1	31	25.2	33.4	28.1
Sex	M	M	F	F	M	M	M
Age	54	53	83	67	26+	70	30

To define accurate boundary conditions, it was necessary to develop an FE model of the buck. The seat and seat back mechanical properties of the buck were characterized via different experiments using an Instron machine (Instron model 8874), and 6 Degree of Freedom (DOF) robotic arm (KUKA Robot, KR300 R2500 Ultra). The Instron machine was used to perform a series of compression tests on the foam cubes extracted from the seat cushion. The KUKA robot used, was equipped with a 6-axis load cell attached to the end effector, which allows for both, force and position control, with a 0.06 mm position accuracy and a 2.5 ms (400 Hz) control loop. A spherical indenter was attached to the robot for calibration and validation tests, (Fig. 2). Indentation tests at varied locations were performed on both the seat and seat back to capture the stiffness. Slide tests, with an indenter wrapped in cloth used for corresponding cadaver tests, at multiple rates and with different normal forces were conducted to measure the friction properties of the seat. Then, the seat, seat back, frame, and seat reinforcement structure were 3D scanned, and the scan was cleaned, and meshed. Finally, the mechanical properties of the modelled buck components were calibrated and validated based on the experimental tests.

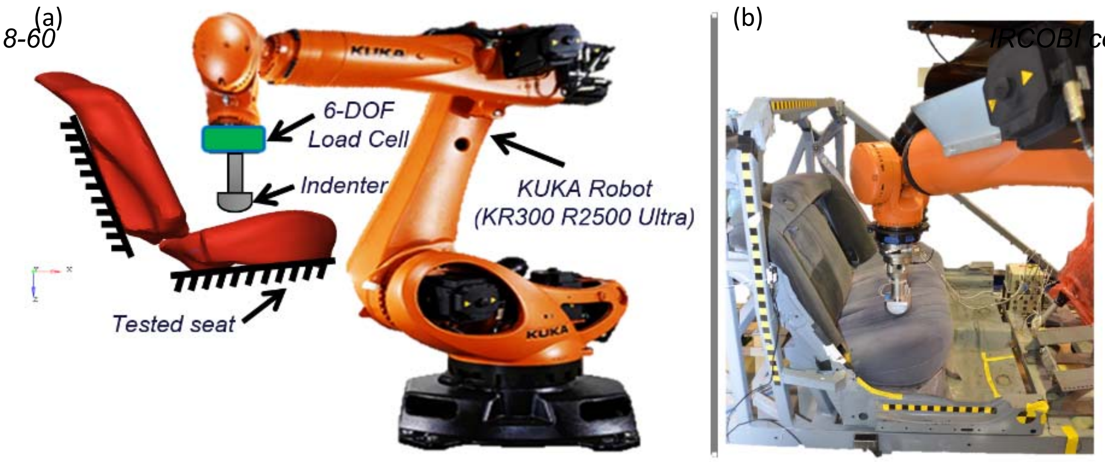

Fig. 2. Robotic arm setup for seat testing, a) test schematic with used indenters, b) actual test setup.

Afterwards, the 70 years old GHBMC with the height of 188 cm height and BMI of 35 kg/m^2 was positioned in the seat to match the corresponding PMHS (Fig. 3). Positioning simulation was performed through several steps aimed to match the femur angle, tibia angle, H-point, torso angle (an angle between the horizontal plane and the line connecting the greater trochanter and the acromion) and position of the occupant's arms. Next, the restraint system model was developed. The model of the actual retractor used in the PMHS sled tests with pre-tensioner and force limiter was obtained from the original equipment manufacturer supplier and implemented into the model. The seat belt was modelled using the 2D shell seat belt formulation. Since it was expected that the modelled restraint system would need to facilitate a large belt payout, 2D shell sliprings were used to provide a more stable and robust representation of belt webbing routing. Finally, the buck model was subjected to the acceleration pulse recorded during the 48 km/h PMHS experiment.

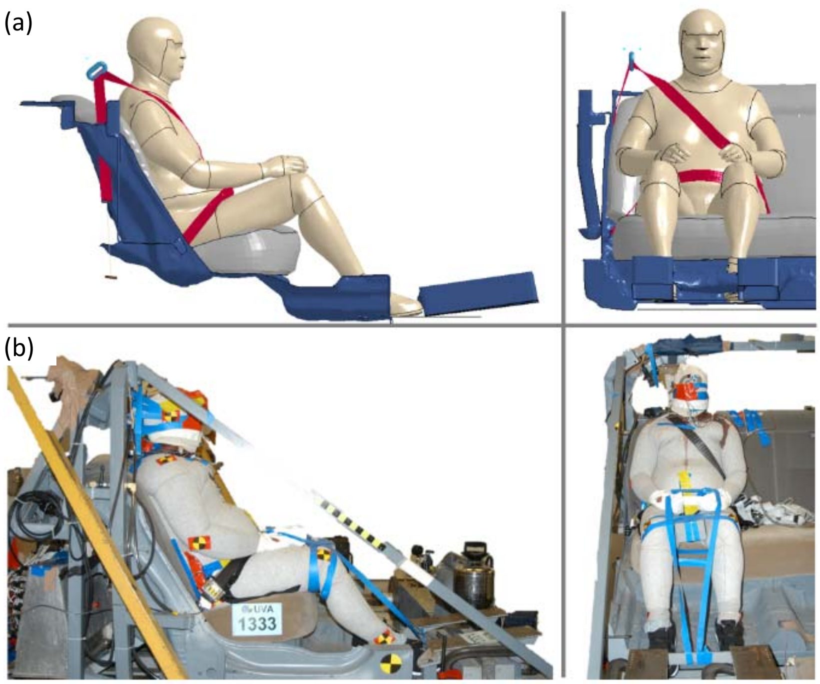

Fig. 3. Obese occupant positioned in a rear seat buck, a) FE model, b) PMHS test (images from study described in [11]).

Belt Pull Test Simulations

The second part of this study was aimed at evaluating the biofidelity of obese GHBMC models by comparing the model responses with the obese PMHS in a series of belt pull tests previously performed at the UVa-CAB [20]. This task was not aimed at validating the model, since this would require morphing of the model to match the PMHS, but rather at evaluating whether the obese occupant models can generally represent similar behaviour as the PMHS. Out of the two PMHSs tested, the PMHS with a BMI of 31 kg/m^2, height of 1,650 mm and weight of 84.4 kg was chosen for comparison with the 30 years old GHBMC obese model with a height of 1,750 mm and a BMI of 30 kg/m^2 (Fig. 1, Table 1).

A FE model of the test fixtures used in the belt pull tests was developed using 3D drawings of the original test fixture. All parts were modelled as rigid bodies. A belt pulling piston along with the 1D belt routed through the series of sliprings was connected to the 2D belt webbing positioned on the occupant. Following the test setup, the obese GHBMC model was secured to the test fixture through spine mounts connected to every other vertebra. A prescribed force time history, recorded from the experiment, was applied to the belt pulling piston in order to force the belt into the occupant's abdomen (Fig. 4).

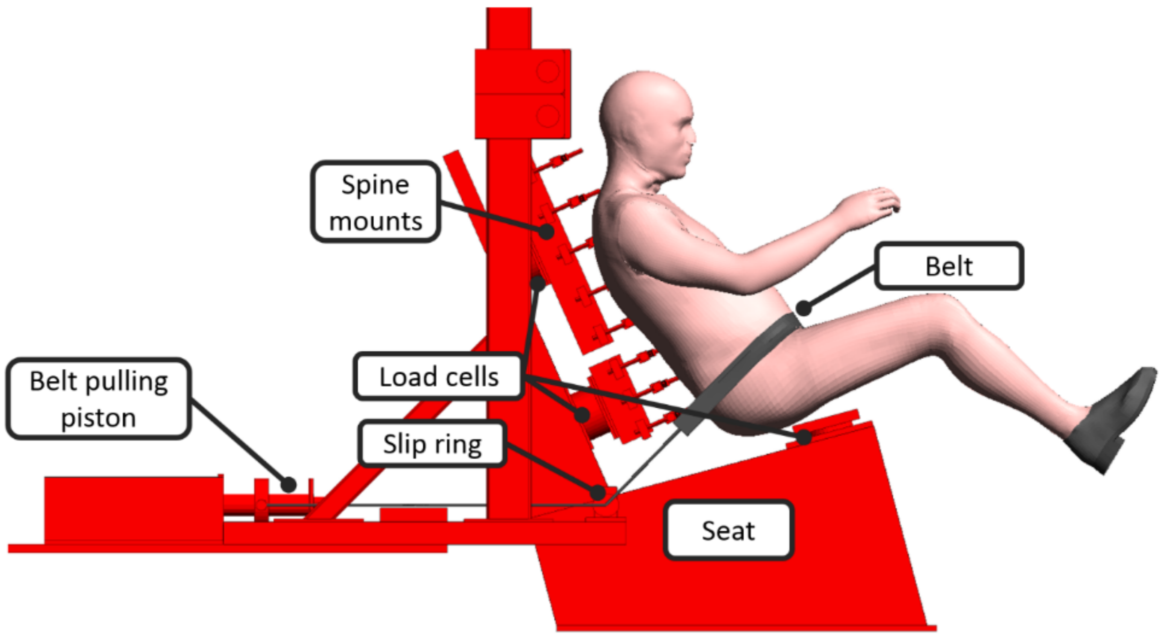

Fig. 4. FE model of the belt pull test setup

The best effort was made to position the obese GHBMC model according to the initial position of the PMHS. However, due to geometrical differences between the two, some uncertainty remained. First, even though both had a BMI close to 30 kg/m^2, they differed in stature and weight. Second, the tested PMHS was a female, whereas all of the obese GHBMC models were male. To unify the positioning procedure, the pelvic plane, defined by the points on left and right ASIS (ASISL and ASISR) and pubic symphysis was established for both PMHS and GHBMC. Two different models were developed for the obese GHBMC in order to evaluate the variability of the model response with respect to the initial position. First, a model matching the position and alignment of the pelvic plane was created. However, the two differed in the lumbar spine alignment. As a result, a second model was created through a rotation of the pelvis to match the alignment of the lumbar and thoracic spine (Fig. 5a).

Reference [20] showed that belt motion over the pelvis while penetrating the abdominal flesh and the submarining-like belt kinematics was highly dependent on the initial position of the belt relative to ASIS. The authors observed that if the belt pulling force vector, drawn from the belt initial position, points in the direction above the ASIS the belt is likely to slip over the iliac crest and into the abdomen. However, when the same vector points below the ASIS the belt is likely to remain anterior to the pelvis and engage with the bony structure of pelvis. Consequently, three different initial positions for the belt were considered (Fig. 5b).

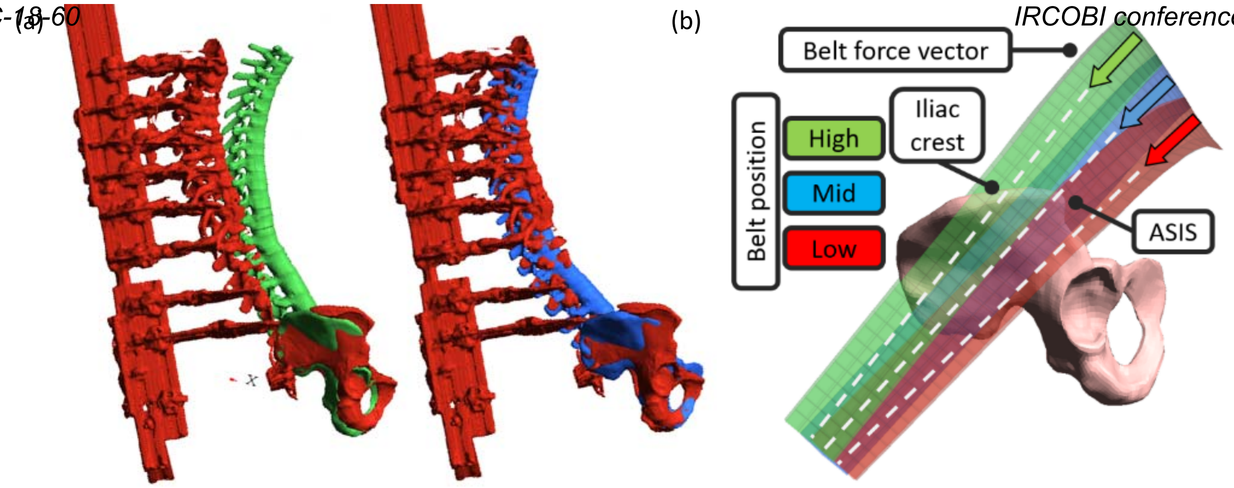

Fig. 5. HBM and belt positioning for the belt pull tests, a) models considering pelvis (far left) and spine alignment (middle), and, b) lap belt initial positions relative to the pelvis.

Tissue Level Tests

The third part of this study was aimed at evaluating the material properties used for the abdominal flesh in the GHBMC model. Over last two decades there have been multiple studies [21-32] characterizing adipose tissue in a variety of loading conditions. Since several of these studies utilized tests with low strain values, lacked shear test data, which was hypothesized to be critical for the purpose of this study, or utilized previously frozen human or animal tissue, the results from [31] were used as the basis for the comparison. Reference [31] performed multiaxial mechanical testing and constitutive modelling of human adipose tissue. The results of shear tests on the fresh human subcutaneous adipose tissue were used as one of the test setups in this study. For the purpose of this study a FE simulation of an 8 x 8 x 8 mm cube of GHBMC model abdominal flesh was created matching the loading and boundary conditions of the published test. Fig. 6 shows the 10 x 10 x 10 element cube of the adipose tissue material subjected to shear test as described in [31]. Since the HBM material model used for flesh did not account for rate effects, results from only one loading rate were compared with the experimental results.

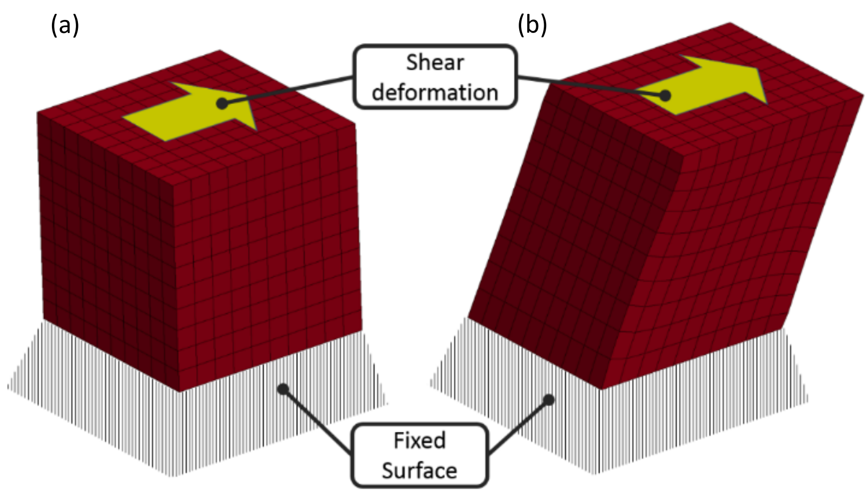

Fig. 6. A cube of GHBMC adipose tissue material subjected to shear test as described in [31]

FE Software and Hardware Used

The LS-DYNA (LSTC, Livermore, CA, USA), R9.1.0, Distributed Memory Parallel (MPP) version with explicit solver was used to perform all simulations involving obese GHBMC models. These simulations were performed using the UVA's state-of-the-art *Rivanna* HPC computational cluster, which is a ~5,000 core (Intel Xeon E5-2670v2, 2.5 GHz, 20 core) university-wide resource. Tissue level test simulations were carried out using a PC machine with LS-DYNA, R9.1.0, Shared Memory Processing (SMP) version with the explicit solver.

III. RESULTS

Sled Test Simulations

The head, shoulder, pelvis, and knee trajectories (displacement with respect to the buck), as well as the torso angle time history of the obese model, were compared with those of the obese PMHS. Fig. 7a shows the trajectory of different body segments of the obese GHBMC and PMHS. The lines connecting the head to the shoulder, and the shoulder to the pelvis are illustrated at four different time points: t= 0 ms, t= 58 ms, t= 87 ms, and t= 117 ms. The torso angle was defined as the an angle between the horizontal plane and the line connecting the greater trochanter and the acromion (Fig. 7b).

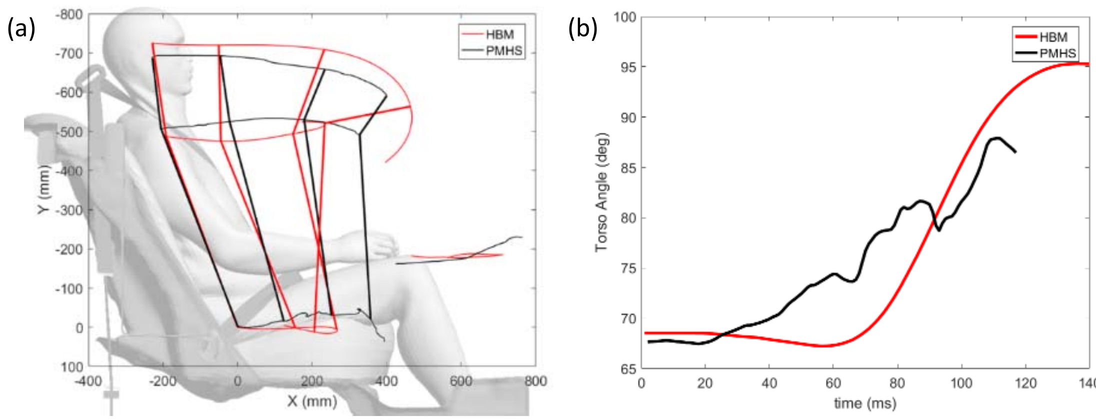

Fig. 7. Sled test results, a) trajectory of different body segments, b) occupant torso angle (HBM vs PMHS) [19].

Similar to the PMHS tests, the obese HBM experienced a significant lower extremity forward motion, which was a result of increased mass and delayed engagement of the pelvis due to the increased thickness of adipose tissue. Nevertheless, the obese model was not able to exhibit submarining (pelvis sliding under the belt as the belt slides over the iliac crest and loads the abdomen) as opposed to the PMHS. In the PMHS test, the lap belt did not engage with the bony structure of the pelvis. This resulted in the belt sliding above the pelvis and into the abdomen of the PMHS. Consequently, the subject exhibited undesirable kinematics during the sled run, with the torso never pitching as far forward as the obese GHBMC model throughout the run (Fig. 7b). However, with the obese GHBMC model, the lap belt remained anterior to the ASIS and remained engaged with the pelvis, hence it constrained the pelvis motion throughout the whole sled run. In addition, while the torso angle of the obese PMHS remained less than 90 degrees, the torso of the obese model pitched past 90 degrees towards the end of the run (Fig. 7).

Belt Pull Test Simulations

Both GHBMC initial positions developed for the belt pull test (Fig. 5) showed no noticeable difference in the results. Therefore, for brevity, only the results from the belt pull with the spine aligned model are presented in this section. Fig. 8 shows the comparison of webbing trajectories obtained from the experiment and the simulation. In both cases, the time histories for points on the webbing directly anterior to ASISL and ASISR were extracted and plotted over the experimental results. Trajectories for low, middle and high initial belt positions are shown. Both low and middle initial belt positions resulted in the webbing engaging the pelvis either below (Low), or at the ASIS (Mid). Belt in the high initial position followed the initial trajectory observed in the experiment, sliding over the ASIS. However, it failed to slide over the iliac crest and into the abdomen (Fig. 8).

Since the selected GHBMC model differed from the target PMHS in anthropometry, specifically in the amount of tissue covering the pelvis, it was speculated that a larger belt pull force is required to force the belt over the iliac crest and into the abdomen. For that purpose, the simulation with a high belt initial position and doubled force input was carried out (High-DF). The results showed that the belt again followed the initial belt trajectory observed in the experiment. However, it failed to slide into the abdomen (Fig. 8).

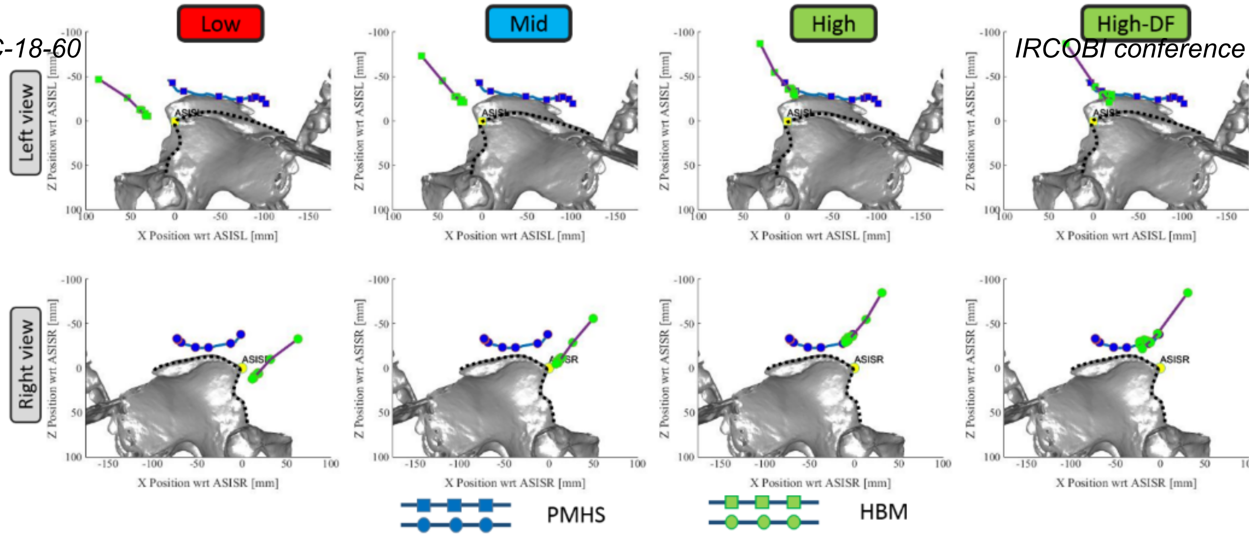

Fig. 8. Belt pull test results. Webbing trajectories obtained for low (Low), middle (Mid), high (High), and high with double belt force input (High-DF) webbing initial positions (HBM vs PMHS).

Tissue Level Tests

Lastly, simulation of the adipose tissue shear test illustrated that the material model used to represent the HBM flesh is approximately one order of magnitude stiffer than human abdominal subcutaneous adipose tissue (Fig. 9). Reference [21] observed that human abdominal adipose tissue can be characterised as a nonlinear anisotropic and viscoelastic material. However, none of the experimental responses matched the shear response obtained from the GHBMC material model.

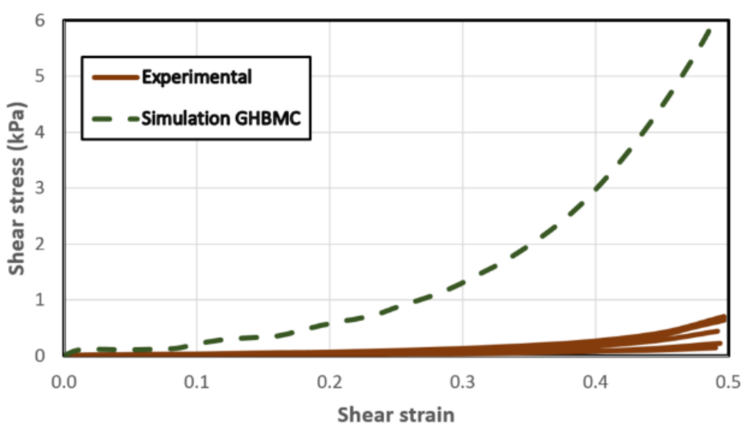

Fig. 9. Shear test response of the abdominal adipose tissue. Experiment [21] vs GHBMC adipose tissue model results.

IV. Discussion

To our knowledge, this is the first study to perform a detailed comparison of obese GHBMC model predictions to available test data. A multi-scale comparison that included whole-body kinematic and kinetic responses in sled tests, pelvis-belt interaction in belt pull tests, and material response in tissue-level testing was performed.

The superficial adipose tissue has a substantial effect on restraint system interaction, and the resulting occupant kinematics, during motor vehicle crashes. First, adipose tissue influences webbing routing, which often results in a limited, or lack of pelvic engagement by the restraint system [11]. Second, it increases the distance between the lap belt and skeletal structure [13]. Both of these effects may increase the risk of lap belt penetration into the abdomen, resulting from large superficial tissue deformations when the occupant loads the restraint system. As a result, the material model used to describe the mechanical response of the adipose tissue in an FE model plays a critical role in occupant/restraint interaction predicted with that model.

The obese GHBMC model successfully replicated several characteristics of occupant responses observed in the experiments. Model simulations showed substantial lower extremity forward motion, which was the result of increased mass and delayed engagement of the pelvis caused by the increased thickness of adipose tissue. However, the model failed to replicate the submarining behaviour observed in the PMHS tests. Throughout the simulation, the webbing remained engaged with the iliac wings and it remained anterior to the pelvis. As a result, a substantial difference in torso angle and restraint system engagement was observed between the experiment and the simulation. A similar response was observed during belt pull simulations. The obese GHBMC model failed to replicate the webbing trajectory observed during the experiments, where it slid over the iliac crest and into the abdomen. Even with the increased belt pull force the webbing remained constrained in the proximity of the ASIS. It should be noted, however, that in both of the PMHS experiments no belt slippage relative to the occupant skin/flesh was observed, and consequently, the motion of the webbing up and over the ASIS and into the abdomen was the result of shearing deformation of the pelvic/abdominal flesh. As a result, we concluded that the difference in the occupant response is likely associated with the abdominal flesh formulation.

With these observations in mind, it was theorised that the GHBMC flesh material model along with the current mesh formulation results in the overly stiff response when used to represent human adipose tissue. A belt pull test serves as a good explanation for this hypothesis (Fig. 10). When the belt is initially pulled with a force F_B it compresses the adipose tissue over the pelvis (Fig. 10a). Next the webbing encounters the bony structure of the pelvis which provides a reaction force F_p (Fig. 10b). If, at this point, the webbing is superior to the ASIS, the resultant of these two forces will pull the belt over the iliac crest and into the abdomen (Fig. 10c). However, if the flesh model is overly stiff in shear, then the resultant of the belt and pelvis forces could be carried by the flesh and prevent the belt from sliding over the iliac wing.

Consequently, the biofidelity of the GHBMC abdominal flesh material model was evaluated by simulating some material-level test data from the literature. The test data illustrated that the material used to model the flesh of the GHBMC was approximately an order of magnitude stiffer under shear loading. Currently there are several studies available where authors used the available test data to formulate biofidelic material models for adipose tissue that could be used with the available HBMs [33, 34]. It is possible that a lower shear stiffness could result in greater motion of the lap belt relative to the pelvis. This in turn could allow the model to submarine and improve its biofidelic predictions. Similar findings have been previously shown by [22], where authors needed to modify the GHBMC's flesh properties in order to match the response with the PMHS belt pull results.

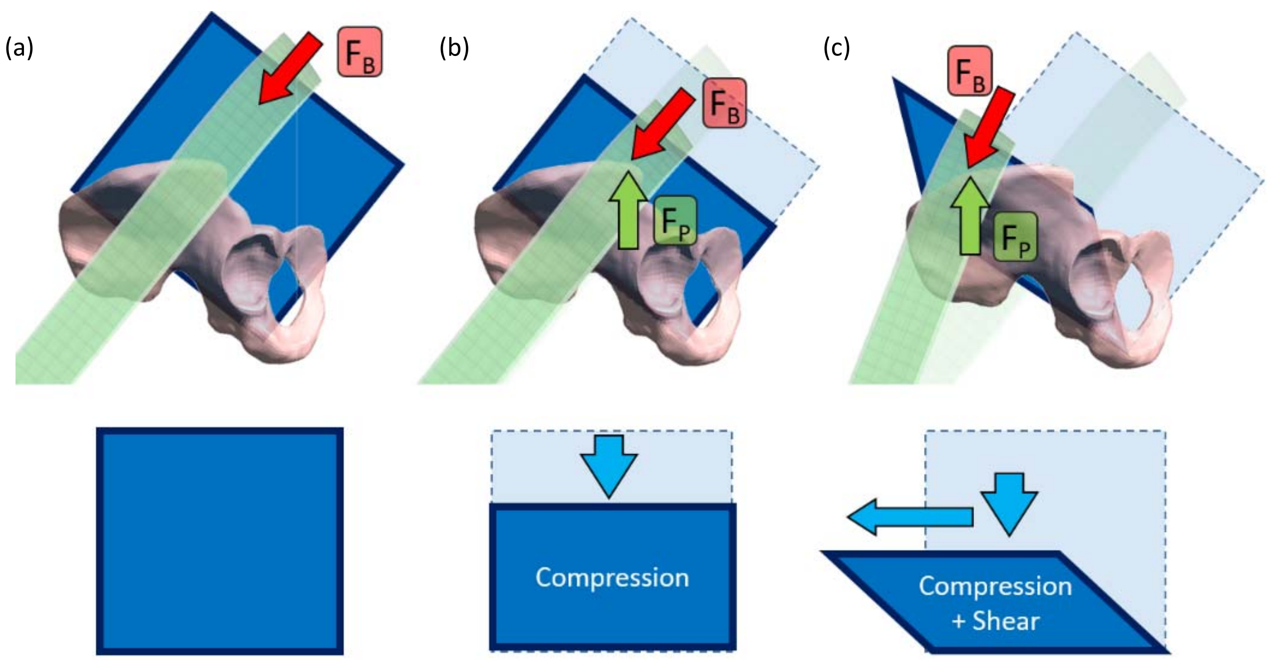

Fig. 10. Mechanism of webbing motion in belt pull tests, F_B – force from the webbing, F_P – reaction force from the pelvis. a) Initial webbing positioning with undeformed abdominal flesh, b) compression of the abdominal flesh over the pelvis, c) compression and shearing of the abdominal flesh and webbing sliding over the iliac crest.

Additionally, it is possible that the current Lagrangian mesh formulation implemented in the obese GHBMC models might prove challenging for accurate adipose tissue modelling. Since these models were developed by morphing the FE mesh of M-50 model, certain areas of the obese models featured very coarse mesh. Fig. 11 shows a cross section along the sagittal plane where the three-element-thick abdominal external flesh part has been morphed to accommodate the geometrical differences between the BMI 25 and BMI 35 occupant.

Additionally in a Lagrangian element formulation, the domain spatial discretisation (mesh) is permanently bound to maintain the material (mass) particles originally assigned to each element. Simply said, the FE mesh follows the material deformation and no mass transfer (advection) between the neighbouring elements is possible. As a result, substantial deformation of the material causes the Lagrangian elements to stretch, lose the desired aspect ratio, negatively impact the simulation time-step, suffer from excessive hourglassing, and force premature termination. Consequently, several complementary simulations, aimed at exploring the sensitivity of the model response (varied occupant position or belt pull force), failed to run to completion due to negative volume errors in the abdominal tissue.

Due to the fluid like properties of adipose tissue including a large bulk modulus (approaching incompressibility), low shear modulus, and the ability to undergo very large deformation, this tissue may be better modelled as a fluid. This approach could improve the stability and robustness of the modelled adipose tissue. Currently there are multiple formulations available in FE solvers that could be considered for this application including Arbitrary Lagrangian-Eulerian (ALE), Smooth Particle Hydrodynamics (SPH), Smooth Particle Galerkin (SPG), and other meshless methods. All of the proposed methods provide a potential solution to a large distortion problems either through allowing the advection between elements (ALE) or through eliminating FE mesh altogether. Investigating the appropriateness of these methods is a natural next step to address the biofidelity of the adipose tissue material.

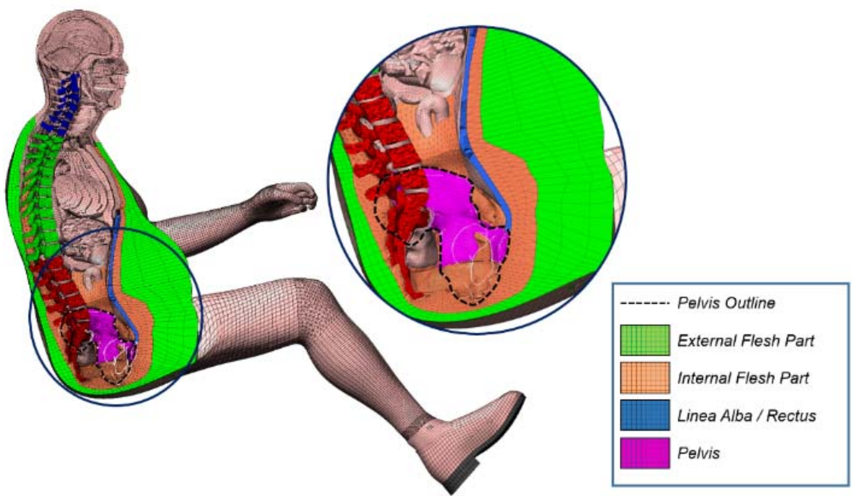

Fig. 11. Mesh and tissue allocation around the occupant's pelvis. Sagittal plane cross section through the obese GHBMC, BIM 35, 188 cm, 70 years old model.

It is worth noting that the HBMs used in this study were not morphed to match the exact anthropometries of corresponding PMHSs. In case of the sled test, a statistical shape modelling tool was used to generate a model whose height and weight (BMI) matched the target PMHS. Nevertheless, there might be other measures, i.e., adipose tissue distribution, which could be different between the two targets [17]. In case of the belt pull tests a model with a different height and weight, but matching BMI was used. This resulted in differences in abdominal shapes, and initial webbing positions between the HBM and PMHS. In order to account for these differences, several simulations with varied belt pull force and belt initial position were performed. Although these geometrical discrepancies are limitation of this study, the models failed to replicate the general trends that were expected based on the previous PMHS studies.

V. CONCLUSIONS

The following conclusions can be drawn from this study:

1) The obese GHBMC models failed to replicate the submarining behaviour, and restraint kinematics, observed in the PMHSs in rear-seat sled tests.
2) The obese GHBMC models failed to replicate the belt trajectory observed in the belt pull tests; belt sliding up over the iliac wings and into the abdomen.
3) The GHBMC flesh material model exhibits a much stiffer stress/strain response in shear compared to

human abdominal subcutaneous adipose tissue data from the literature.

The obese HBMs could be useful tools to further understand the obese occupant response in crashes and to investigate the challenges in, and strategies for, developing an effective restraint system for this population. However, modification of adipose tissue mechanical properties may be required to improve the biofidelity of the models. It seems that it is the shearing behaviour of the abdominal flesh that permits the submarining seen in the sled tests and the belt slip and abdominal loading seen in the belt pull tests. Since it is likely that belt/pelvis/abdomen interaction is responsible for at least some of the increased injury risk for obese occupants, biofidelic belt-to-pelvis interaction is paramount for the injury risk evaluation and countermeasure development. The results of this study suggest that improved models of abdominal flesh, and specifically subcutaneous adipose tissue, should be developed and implemented to examine their effect on pelvis/belt/abdomen interaction before utilising obese HBMs to predict injury risks to obese occupants in crash simulations.

VI. Acknowledgment

This study was supported by the National Highway Traffic Safety Administration (NHTSA) by DTNH2215D00022-0004. Views or opinions expressed or implied are those of the authors and are not necessarily representative of the views or opinions of the NHTSA.

VII. References

[1] World Health Organization. Obesity and overweight. Fact sheet. Reviewed February 2018. Internet: http://www.who.int/mediacentre/factsheets/fs311/en/ Date updated April 2018.

[2] Mock, C. N., Grossman, D. C., Kaufman, R. P., Mack, C. D., & Rivara, F. P. (2002) The relationship between body weight and risk of death and serious injury in motor vehicle crashes. Accident Analysis & Prevention, 34(2), 221-228.

[3] Zhu, S., Layde, P. M., Guse, C. E., Laud, P. W., Pintar, F., Nirula, R., & Hargarten, S. (2006) Obesity and risk for death due to motor vehicle crashes. American journal of public health, 96(4), 734-739.

[4] Viano, D. C., Parenteau, C. S., & Edwards, M. L. (2008) Crash injury risks for obese occupants using a matched-pair analysis. Traffic injury prevention, 2008, 9(1), 59-64.

[5] Jehle, D., Gemme, S., & Jehle, C. (2012) Influence of obesity on mortality of drivers in severe motor vehicle crashes. The American journal of emergency medicine, 30(1), 191-195.

[6] Choban, P. S., Weireter Jr., L. J., & Maynes, C. (1991) Obesity and increased mortality in blunt trauma. Journal of Trauma and Acute Care Surgery, 31(9), 1253-1257.

[7] Brown, C. V., Neville, A. L., Rhee, P., Salim, A., Velmahos, G. C., & Demetriades, D. (2005) The impact of obesity on the outcomes of 1,153 critically injured blunt trauma patients. Journal of Trauma and Acute Care Surgery, 59(5), 1048-1051.

[8] Boulanger BR, Milzman D, Mitchell K, Rodriguez A. (1992) Body Habitus as a Predictor of Injury Pattern After Blunt Trauma. Journal of Trauma, Vol. 33, No. 4, pp 228-232.

[9] Neville AL, Brown CV, Weng J, Demetriades D, Velhamos GC. (2004) Obesity is an Independent Risk Factor of Mortality in Severely Injured Blunt Trauma Patients. Arch. Surg., Vol. 139, pp 983- 987.

[10]Jakobsson L, Lindman M. (2004) Does BMI (Body Mass Index) Influence the Occupant Injury Risk Pattern in Car Crashes? I*n Proceedings of the IRCOBI Conference*, pp 427-430. 2004. Graz, Austria.

[11]Forman, J., Lopez-Valdes, F. J., Lessley, D., Kindig, M., Kent, R., & Bostrom, O. (2009) The effect of obesity on the restraint of automobile occupants. In Annals of Advances in Automotive Medicine/Annual Scientific Conference, (Vol. 53, p. 25).

[12]Kent, R. W., Forman, J. L., & Bostrom, O. (2010) Is there really a “cushion effect”?: a biomechanical investigation of crash injury mechanisms in the obese. Obesity, 18(4), 749-753.

[13]Reed, M. P., Ebert-Hamilton, S. M., & Rupp, J. D. (2012) Effects of obesity on seat belt fit. Traffic injury prevention, 13(4), 364-372.

[14]Turkovich, M., Hu, J., van Roosmalen, L. and Brienza, D. (2013) Computer simulations of obesity effects on occupant injury in frontal impacts. International journal of crashworthiness, 18(5), pp.502-515.

[15]Shi, X., Cao, L., Reed, M. P., Rupp, J. D., & Hu, J. (2015) Effects of obesity on occupant responses in frontal crashes: a simulation analysis using human body models. Computer methods in biomechanics and biomedical

engineering, 18(12), 1280-1292.

[16]Wang, Y., Bai, Z., Cao, L., Reed, M. P., Fischer, K., Adler, A., & Hu, J. (2015) A simulation study on the efficacy of advanced belt restraints to mitigate the effects of obesity for rear-seat occupant protection in frontal crashes. Traffic injury prevention, 16(sup1), S75-S83.

[17]Hu, J., Fanta, A., Neal, M. O., Reed, M. P., Wang, Y. (2016) Vehicle crash simulations with morphed GHBMC human models of different stature, BMI, and age. Proceedings, 4th International Digital Human Modeling Conference. 2016. Montreal, Canada.

[18]Kitagawa, Y., Hayashi, S. and Yasuki, T. (2017) Comparison of Impact Kinematics between Non-obese and Obese Occupants in Frontal and Lateral Impacts. *In IRCOBI Conference Proceedings,* 2017. Antwerp, Belgium.

[19]Joodaki, H., Forman, J., Forghani, A., Overby, B., Kent, R., Crandall, J., ... & Bostrom, O. (2015) Comparison of Kinematic Behaviour of a First Generation Obese Dummy and Obese PMHS in Frontal Sled Tests. *In IRCOBI Conference Proceedings*, (No. IRC-15-57). 2015. Lyon, France

[20]Kim, T., Park, G., Montesinos, S., Subit, D., Bolton, J., Overby, B., ... & Kim, H. (2015) Abdominal Characterization Test Under Lap Belt Loading. *In 24th International Technical Conference on the Enhanced Safety of Vehicles (ESV)*, (No. 15-0312). 2015. Gothenburg, Sweden

[21]Alkhouli N, Mansfield J, Green E, Bell J, Knight B, Liversedge N, Tham JC, Welbourn R, Shore AC, Kos K, Winlove CP. (2013) The mechanical properties of human adipose tissues and their relationships to the structure and composition of the extracellular matrix. American Journal of Physiology-Endocrinology and Metabolism. Oct 8;305(12):E1427-35.

[22]Comley, K., & Fleck, N. A. (2010). A micromechanical model for the Young's modulus of adipose tissue. International Journal of Solids and Structures, 47(21), 2982-2990.

[23]Comley, K., & Fleck, N. (2012). The compressive response of porcine adipose tissue from low to high strain rate. International Journal of Impact Engineering, 46, 1-10.

[24]Geerligs, M., Peters, G. W., Ackermans, P. A., Oomens, C. W., & Baaijens, F. (2008). Linear viscoelastic behavior of subcutaneous adipose tissue. Biorheology, 45(6), 677-688.

[25]Geerligs, M., Peters, G. W., Ackermans, P. A., Oomens, C. W., & Baaijens, F. P. (2010). Does subcutaneous adipose tissue behave as an (anti-) thixotropic material?. Journal of biomechanics, 43(6), 1153-1159.

[26]Gefen, A., & Haberman, E. (2007). Viscoelastic properties of ovine adipose tissue covering the gluteus muscles. Journal of biomechanical engineering, 129(6), 924-930.

[27]Iatridis, J. C., Wu, J., Yandow, J. A., & Langevin, H. M. (2003). Subcutaneous tissue mechanical behavior is linear and viscoelastic under uniaxial tension. Connective tissue research, 44(5), 208-217.

[28]Omidi, E., Fuetterer, L., Mousavi, S. R., Armstrong, R. C., Flynn, L. E., & Samani, A. (2014). Characterization and assessment of hyperelastic and elastic properties of decellularized human adipose tissues. Journal of biomechanics, 47(15), 3657-3663.

[29]Patel, P. N., Smith, C. K., & Patrick, C. W. (2005). Rheological and recovery properties of poly (ethylene glycol) diacrylate hydrogels and human adipose tissue. Journal of biomedical materials research Part A, 73(3), 313-319.

[30]Sims, A. M., Stait-Gardner, T., Fong, L., Morley, J. W., Price, W. S., Hoffman, M., ... & Schindhelm, K. (2010). Elastic and viscoelastic properties of porcine subdermal fat using MRI and inverse FEA. Biomechanics and modeling in mechanobiology, 9(6), 703-711.

[31]Sommer, G., Eder, M., Kovacs, L., Pathak, H., Bonitz, L., Mueller, C., ... & Holzapfel, G. A. (2013). Multiaxial mechanical properties and constitutive modeling of human adipose tissue: a basis for preoperative simulations in plastic and reconstructive surgery. Acta biomaterialia, 9(11), 9036-9048.

[32]Voňavková T, Horný L, Kulvajtová M, Žitný R. (2014) Uniaxial Tensile Test of Perivascular Adipose Tissue. Bulletin of Applied Mechanics. 10(36):11-4.

[33]Naseri, H., Johansson, H., & Brolin, K. (2018). A nonlinear viscoelastic model for adipose tissue representing tissue response at a wide range of strain rates and high strain levels. Journal of biomechanical engineering, 140(4), 041009.

[34]Engelbrektsson, K. (2011). Evaluation of material models in LS-DYNA for impact simulation of white adipose tissue. Master's Thesis, Chalmers University of Technology.

[35]Kim, J., Lee, I., Kim, T., & Kim, H. (2015). Validation of Abdominal Characteristics under Lap-belt Loadings using Human Body Model Morphed to an Obese Female. In Paper No. IRC-15-23, I*n Proceedings of the IRCOBI Conference*. 2015. Lyon, France.

VIII. APPENDIX

Appendix provides detailed information on FE models developed for this study.

Fig. A1 shows the FE model of the rear seat buck developed for this study. The model comprises of rigid buck frame (Fig. A1b), foam cushion and foam seatback (Fig. A1c), seat wire frame (Fig. A1d) and a restraint system (Fig. A1e). Seat wire frame was constrained with the seat cushion using the *CONSTRAINED_BEAM_IN_SOLID keyword available in recent versions of LS-Dyna solver. Table A1 provides details on the element formulation, material models and mesh size used for the developed model of rear seat buck.

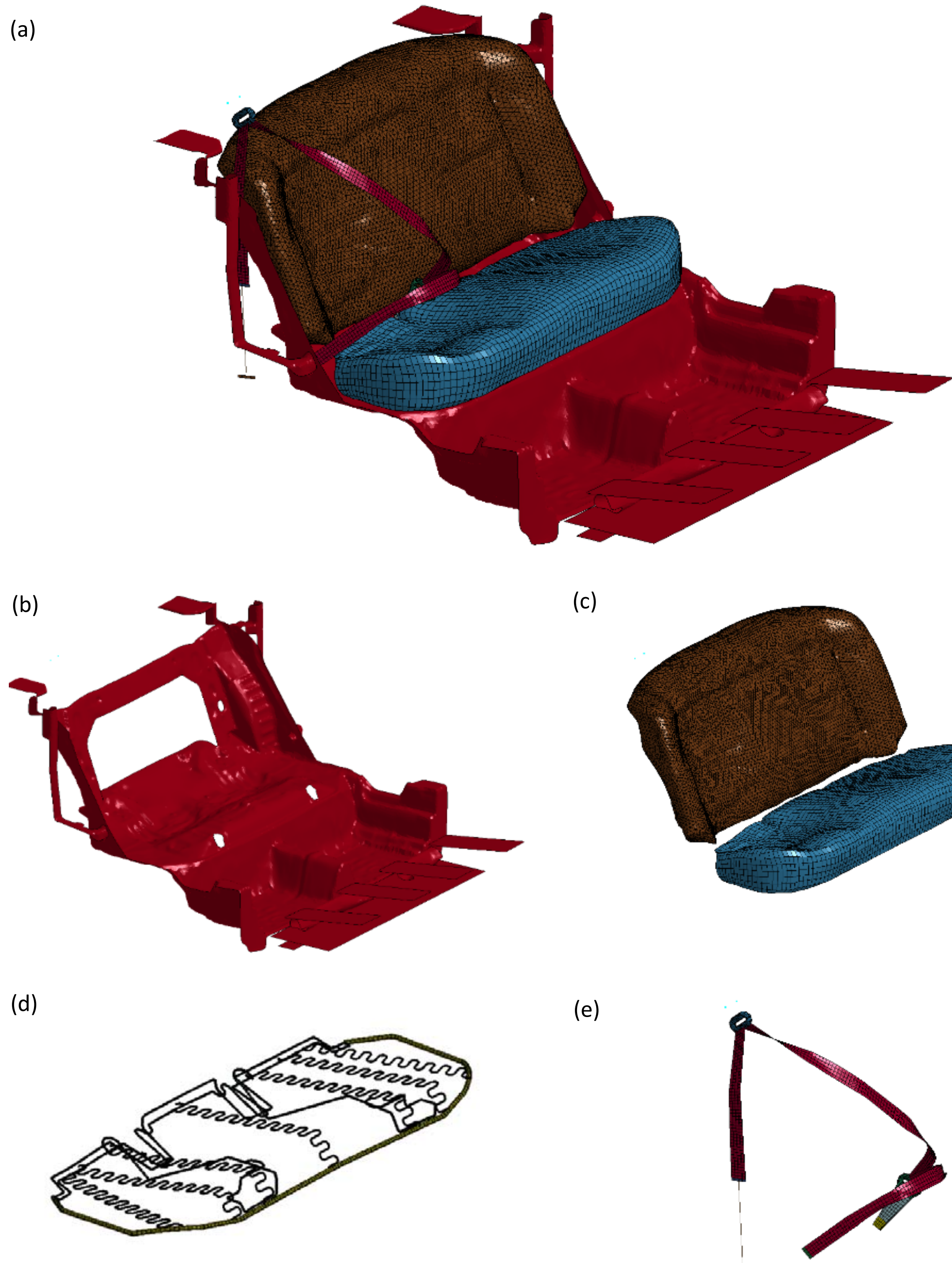

Fig. A1. FE model of the rear seat buck, a) overview of the FE model, b) rigid buck frame, c) foam seat cushion and foam seatback, d) seat cushion frame and d) 3 point belt restraint system.

TABLE A1

Part	Material model	Element Type	ELFORM	No. elements	Average el. Size (mm)
Buck Frame	*MAT_020_RIGID	Shell	2	90267	10
Seat back foam	*MAT_057_LDF	Solid	0	126047	15
Seat cushion	*MAT_057_LDF	Solid	0	13202	20
Seat frame	*MAT_024_PLP	Beam	1	2762	10
Seat belt 1D	*MAT_B01_SEATBELT	1D_Seatbelt	-	28	10
Seat belt 2D	*MAT_B01_SEATBELT_2D	2D_Seatbelt	5	868	10
Belt hardware	*MAT_020_RIGID	Shell	2	1156	10

Fig. A2 shows the FE model of the belt pull test fixture developed for this study. The model comprises of rigid fixture (Fig A2a), and the belt assembly (Fig A2b). The belt assembly was modelled using a series of slip rings along with the 1D seat belt elements connected to a 2D seat belt assembly used to prescribe the load onto the HBM. Table A2 provides details on the element formulation, material models and mesh size used for the developed model of the belt pull fixture.

(a) (b)

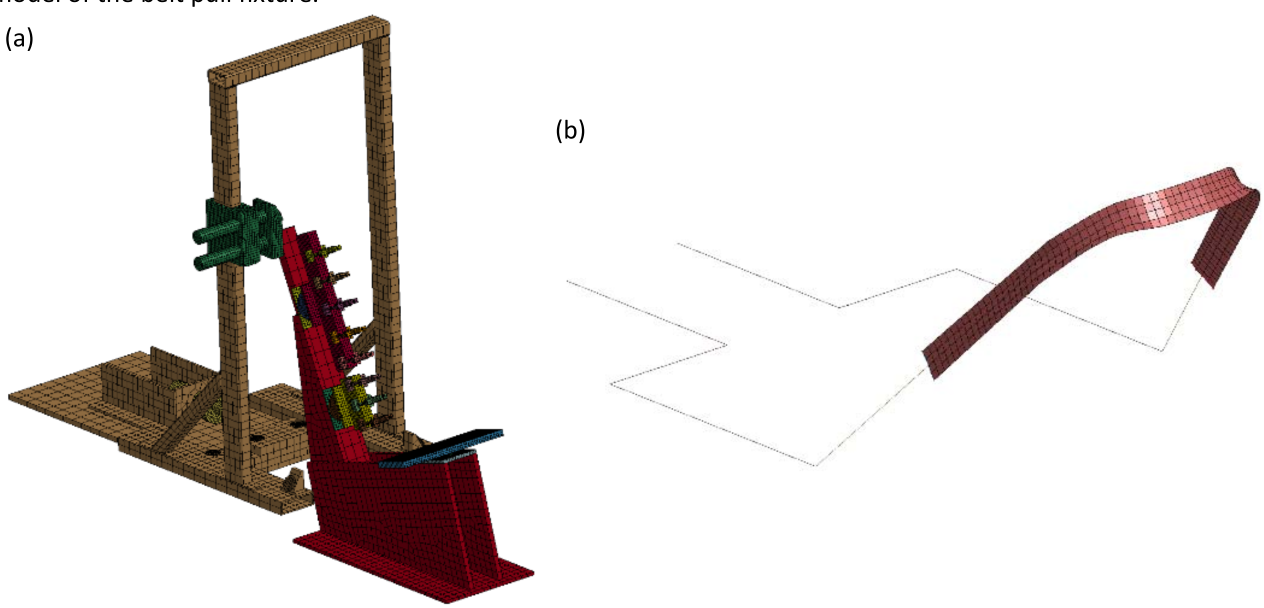

Fig. A2. FE model of the belt pull test buck, a) rigid seat and spinal fixture, b) belt pull system FE model.

TABLE A2

Part	Material model	Element Type	ELFORM	No Elements	Average el. Size (mm)
Seat frame	*MAT_020_RIGID	Solid	1	21355	20
Spine mounts	*MAT_020_RIGID	Solid	1	1087	10
Loading cable	*MAT_B01_SEATBELT	1D_Seatbelt	-	204	10
Seat belt	*MAT_034_FABRIC	Shell	2	324	10